Airflow Patterns through Single Hinged and Sliding Doors in Hospital Isolation Rooms

Article *in* International Journal of Ventilation · September 2015

DOI: 10.1080/14733315.2015.11684074

4 authors:

Petri Kalliomaki
Turku University of Applied Sciences
22 PUBLICATIONS **59** CITATIONS
SEE PROFILE

Pekka Saarinen
Turku University of Applied Sciences
76 PUBLICATIONS **405** CITATIONS
SEE PROFILE

Julian Wei-Tze Tang
University Hospitals Of Leicester NHS Trust
271 PUBLICATIONS **3,992** CITATIONS
SEE PROFILE

Hannu Koskela
Turku University of Applied Sciences
82 PUBLICATIONS **369** CITATIONS
SEE PROFILE

Airflow Patterns through Single Hinged and Sliding Doors in Hospital Isolation Rooms

Petri Kalliomäki[1], Pekka Saarinen[1], Julian W Tang[2,3] and Hannu Koskela[1]

[1]Finnish Institute of Occupational Health, Turku, Finland
[2]Alberta Provincial Laboratory for Public Health, Edmonton, Alberta, Canada
[3]Medical Microbiology and Immunology, University of Alberta, Edmonton, Alberta, Canada

Abstract

Door operation and the subsequent passage of occupants through the doorway can cause containment failures in hospital isolation rooms. Typically hinged doors are used between the isolation room and anteroom/corridor in healthcare facilities. However, sliding doors can reduce door induced airflows through the doorway and hence effectively reduce the contaminant outflow during the door operation.

Airflow patterns through single hinged and sliding doors, in combination with human passage (simulated with a moving mannequin), inside a full-scale hospital isolation room mock-up, were compared. The experiments were carried out in still air (i.e. without ventilation) in order to examine the effect of different factors without the masking effect of ventilation. Smoke visualizations were performed to qualitatively illustrate airflow through the doorway. Tracer gas measurements were carried out to quantify the air exchange between rooms caused by door operation and passage.

Smoke visualization indicated that the sliding door induce a smaller air exchange through the doorway compared to a hinged door. The effect of passage was found to be notable, yet more distinguishable with the sliding door. Airflow volumes through the hinged door varied from 1.2 m^3 to 2.4 m^3 and through the sliding door from 0.3 m^3 to 2.3 m^3, depending on parameter values. The effect of passage was found to be around 0.4 m^3. Although the passage increased the air exchange across the doorway, its effect was relatively much larger for the sliding than for the hinged door.

Key words: isolation room, airflow, airborne infections, doorway, tracer gas, smoke visualization.

1. Introduction

Pandemic outbreaks of airborne infectious diseases such as SARS and influenza A/H1N1 have significantly increased the demand for hospital isolation rooms. Patients with such hazardous and highly contagious diseases are usually placed in negative pressure isolation rooms to prevent further spreading of the disease. However, containment failures happen and the operation of isolation room doors may well be one of the main contributors according to Tang et al (2006). A case study by the same author (Tang et al, 2005) documents one occasion when the operation of isolation room doors has resulted in a containment failure.

A review of experimental studies by Hyttinen et al, (2011) demonstrated that the performance of isolation rooms has been under intense examination. Several studies have assessed the containment effectiveness of such rooms by monitoring the pressure difference of the rooms when the doors are closed (Rice et al, 2001; Saravia et al, 2007; Fraser et al, 1993). However, there are fewer studies about the effect of door-opening motion and passage on the air exchange between the isolation room and anteroom/corridor.

In a full-scale laboratory study by Hayden et al (1998), the effect of door-opening (single hinged and single sliding doors) and manikin passage through the doorway was quantified by using tracer gases. Interestingly they found out that there was no significant difference on the air volume migration through the doorway between hinged and sliding doors when passage occurred. Rydock and Eian (2004) studied tracer migration with a technician exiting an isolation room (door types unknown). They found elevated tracer gas values in the anteroom and also in the corridor. Adams et al (2011) studied the effect of pressure differential on the containment effectiveness. They found that

passage through the door reduced the containment and concluded that the effectiveness was improved when increasing the pressure differentials between the rooms to counteract and reduce the airflows across the doorways (all doors were of hinged type). Nevertheless, Kokkonen et al (2014) found out that up to 1.7 m^3 of air migrated to the anteroom during the passage of a healthcare worker through the doorway (single hinged door).

Flows across the doorway due to the door opening have also been studied by means of scale models. Tang et al (2005) utilized a simple small-scale water tank model to show that the isolation room door induced flows could have caused an exposure of a healthcare worker to airborne varicella zoster virus in a hospital. Indeed, other small-scale studies have also demonstrated that door opening leads to containment failures (Kiel and Wilson, 1989; Eames et al, 2009; Fontana and Quintino, 2014; Hathway et al, 2014). In another, more detailed small-scale study Tang et al (2013) used a small-scale (1:10) water-tank model to visualize the flow patterns across an isolation room doorway with different hinged and sliding door set-ups without ventilation. These experiments demonstrated that a hinged door design generates the greatest amount of air exchange across an isolation room doorway, as compared to sliding doors. Passage through the doorway was found to contribute additional air (or water in their case) exchange across the doorway.

Computational fluid dynamics (CFD) methods for modelling moving objects with time-accurate Large Eddy Simulation (LES) have advanced notably in recent years thus making it compelling to apply these new techniques to practical problems such as door and passage induced flows. For instance, Choi and Edwards (2008) modelled a manikin walking through an open doorway (in the absence of door and ventilation). In a follow up study, Choi and Edwards (2012) utilized a more complex geometry and simulated a manikin walking from dirty area to clean area through a small chamber fitted with two hinged or two sliding doors. The visualizations and results provided by the simulations are very realistic and hence offer an additional tool for studying door opening and passage induced flows.

Common to past experimental studies (Tang et al, 2013 and Hayden et al, 1998 aside) is that they have not compared the differences between hinged and sliding doors. By knowing the optimal door type and values for door operation it might be possible to significantly reduce the transport and the possible exposure to airborne contaminants in adjacent rooms and spaces in healthcare facilities.

In this study baseline tracer gas measurements and smoke visualizations in a full-scale isolation room model were made for single hinged and sliding doors without imposed ventilation. By testing different door operating parameters and considering the effect of passage and its direction, the fundamental effects of each parameter were studied without the masking effect of ventilation and pressure difference etc. typically present in hospital isolation rooms. Hence the containment effectiveness performances of the two different door types for different scenarios were assessed both quantitatively and qualitatively for hospital isolation rooms.

This study was a part of an international project measuring, visualizing and modelling the airflow patterns across isolation room doorways. The project partner institutions, Finnish Institute of Occupational Health (FIOH), Finland, and National University Hospital (NUH), Singapore, studied the airflow patterns using full-scale air (FIOH) and small-scale water models (NUH), with the latter having already published their findings (Tang et al 2013).

2. Methodologies

2.1 The Full-Scale Isolation Room Method

All the experiments in this study were carried out in a full-scale isolation room model. The model was constructed out of airtight and thermally insulated 80 mm thick clean-room elements into a larger laboratory space (see Figure 1A). The model consisted of two identical rooms (1 and 2) separated by a wall with a connecting door in the middle. The rooms were 4.7 m wide, 4.0 m long and 3.0 m high, see Figure 1B for more detailed layout. The rooms were made identical to enable studying the air migration for both door opening and manikin passage directions simultaneously. Inside the model, there was a 5.0 m long motorized rail running embedded on the floor between the rooms, equipped with a small cart carrying a 1.7 m high manikin made out of foamed plastic (Figure 1C). The manikin was wearing a laboratory robe to simulate the outfit of the staff.

In this study two different door types were used, i.e. a single hinged and a sliding door. In both cases, the doorway was 2.06 m high and 1.10 m wide. The

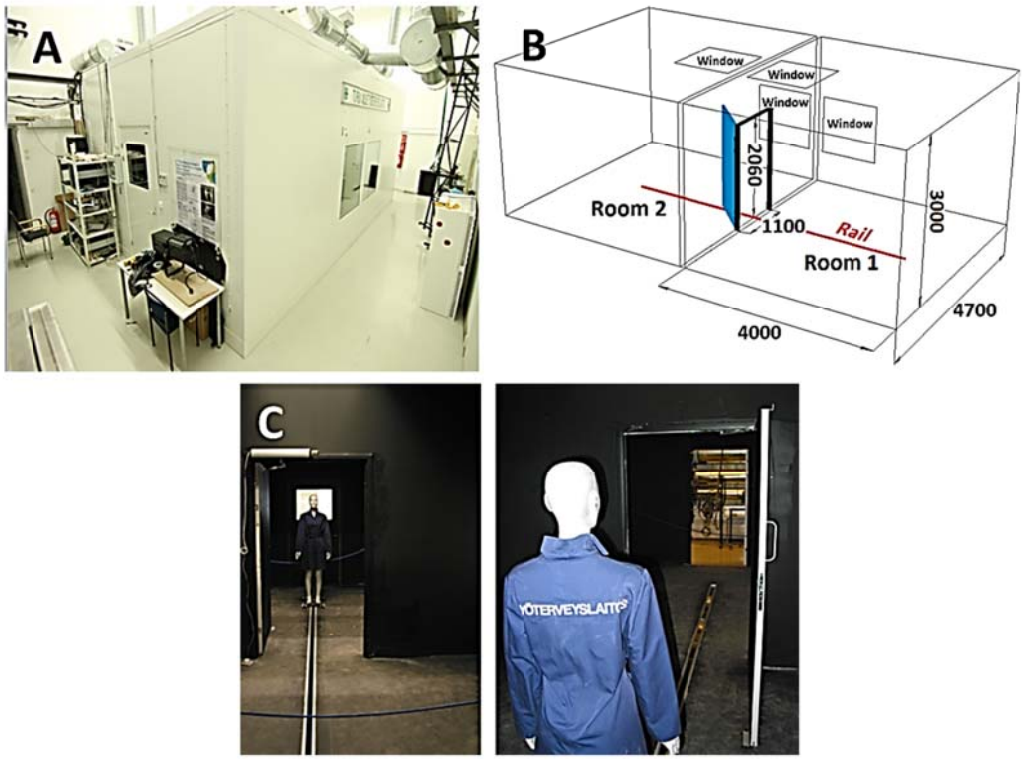

Figure 1. (A) Outside picture of the isolation room model. (B) Layout and dimensions of the model. (C) Inside of the model showing the manikin and the motorized rail.

room into which the hinged door opened was considered as the isolation room. The other room was considered to be the anteroom. Both door types were operated by an automated door operator. Door operation and manikin movement sequences were controlled by a computer program that controlled and varied the door and manikin movement parameters.

There were four thermometers (Craftemp thermistors) inside the isolation room model, two in each of the rooms at 1 m and 2.6 m heights, for monitoring the temperature and possible temperature stratification.

2.2 Smoke Visualizations

Smoke visualizations were undertaken using theatre smoke (Martin Pro-Smoke Super ZRMix) generated using a smoke machine (Martin Magnum 550). The smoke was released into the room via a 4 m long plastic tube. This procedure ensured that the smoke was cooled down before entering the room. The density and the size distribution of the smoke were not measured. However, according to the manufacturer's product support documents (Martin, 2014) the particle size was 1 – 1.5 μm, and was almost neutrally buoyant, thus suitable for airflow pattern visualization.

Inside the room the smoke was mixed with a desk fan. After the smoke was fully mixed, a narrow horizontal or vertical sheet of the empty room was illuminated with theatre spotlights. The distribution fan was shut down about one minute before door operation and recording of the smoke flow through the doorway. Flow visualizations were recorded with a digital camera (Canon 7D, Tokina 11-16 mm lens, full HD video, 1920x1080 px, 25 fps) from four different angles in separate, consecutive experiments) with identical experimental parameters. The smoke machine, camera and lights were positioned outside the isolation room model to decrease interference with the flow through the doorway.

The recorded views included two side and two top-views (from the isolation and anteroom sides). Still images obtained from these videos are presented in this study. A vertical light-sheet (slightly wider than

the door and narrowing towards the lights) was used to illuminate the side-views and a horizontal light-sheet (between 60 cm – 140 cm from the floor also narrowing towards the lights) was used when recording the top-views. The visualizations were carried out only for a certain set of door and passage movement parameters (i.e. door opening time 3 s, hold open time 8 s, closing time 5 s and passage speed 1 m/s) under isothermal conditions.

2.3 Tracer Gas Measurements

2.3.1 Experimental Methods

Tracer gas measurements were used to quantify the total amount of air flowing through the doorway. The effect of the following parameters were examined: passage, door opening time, door hold open time, door total cycle time, door opening angle (gap for sliding door) and 2 °C temperature difference between the rooms (otherwise in isothermal conditions). Due to limitations of the hinged door operator, the closing time (speed) was not an independent parameter but was 1.81 times the opening time. The door parameters were chosen to represent realistic opening and closing times but also so that the held open time was long enough for the manikin to pass through the doorway avoiding collision with the door.

Measurements were made using two tracer gases i.e. sulphur hexafluoride (SF_6) and nitrous oxide (N_2O). This approach enabled the transferred volume to be determined in both directions across the doorway at once. Each of the gases was dosed into different rooms prior to the experiment. The gases were diluted with air before the dosing. Fans in both rooms ensured proper mixing, but were shut down a minute before the door was opened. Samples were drawn into a multigas analyzer (Bruel&Kjaer model 1302) through plastic tubes from three different locations: isolation room, anteroom and surrounding laboratory for background values. Inside the model, perforated sampling tubes ran across the rooms (about 90 cm above the floor) enabling uniform sampling and reducing the possible effect of concentration gradients. The samples were taken from the three locations, serially, at one and a half minute intervals, thus ensuring adequate flushing of the sampling tubes before the next sample was taken from another location.

Each experimental set-up consisted of multiple door openings (5 – 12 depending on the case). The openings were separated by 45 minutes. After all the openings were performed the tracer gases were flushed away from the rooms before a new measurement with different parameter values was started. The manikin moved according to a preset computer program in which it accelerated rapidly to full speed (1 m/s), halted in front of the door and waited for the door to open fully. Then it went through the doorway to the other room after which the door closed. After a wait of about 45 minutes the procedure was performed in the other direction. Typically the experiments included 5 or 6 cycles as described above (manikin back and forth through the doorway). The rooms were then flushed and set up for the next case. These measurements were carried out both with hinged and sliding doors.

2.3.2 Data Analysis

The analysis of the tracer gas measurements was based on the hypothesis of a closed system. This assumption was well justified since no ventilation was involved and the isolation room model was made of airtight elements. According to mass conservation of the gases:

$$\begin{cases} \Delta C_{A,2} V_2 = C_{A,1} X_1 - C_{A,2} X_2 \\ \Delta C_{B,1} V_1 = C_{B,2} X_2 - C_{B,1} X_1 \end{cases}, \quad (1)$$

where X_1 (X_2) is the volume [m^3] migrating from the anteroom (isolation room), V_1 (V_2) the anteroom (isolation room) volume [m^3], $C_{A.1}$ ($C_{A,2}$) the anteroom (isolation room) N_2O concentration prior to the door opening [ppm], $C_{B,1}$ ($C_{B,2}$) the anteroom (isolation room) SF_6 concentration prior to the door opening [ppm], $\Delta C_{A,2}$ the N_2O concentration change [ppm] in the isolation room (prior to and after the door operation) and $\Delta C_{B,1}$ the SF_6 concentration change [ppm] in the anteroom prior to and after the door operation. Solving for X_1 and X_2 gives:

$$\begin{cases} X_1 = \dfrac{C_{B,2}\Delta C_{A,2} V_2 + C_{A,2}\Delta C_{B,1} V_1}{C_{A,1} C_{B,2} - C_{A,2} C_{B,1}} \\ X_2 = \dfrac{C_{B,1}\Delta C_{A,2} V_2 + C_{A,1}\Delta C_{B,1} V_1}{C_{A,1} C_{B,2} - C_{A,2} C_{B,1}} \end{cases} \quad (2)$$

Equation (2) also states that the rooms can have any initial value of the tracers prior to the door operation thus several door openings can be carried out in succession without flushing the rooms.

In reality the system is not absolutely sealed and a small amount of the gases escapes the system due to

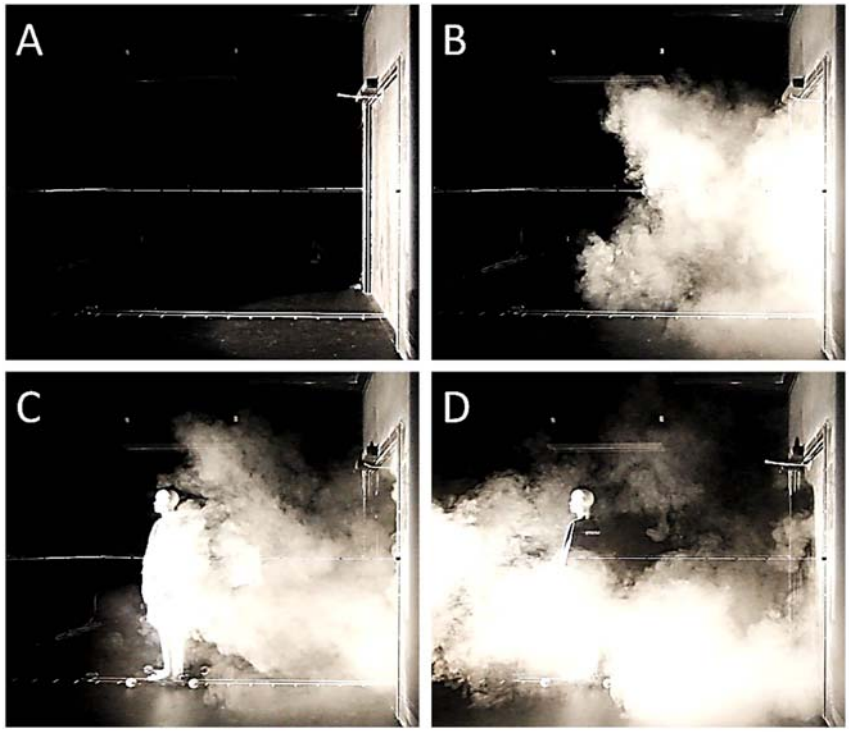

Figure 2. Smoke visualization (anteroom side-view) of the airflow patterns across the doorway generated by the single hinged door and the manikin passage.

the sampling. However, this is so slow that it can be neglected in this case. Also note that when the manikin passes the doorway, the air volume displaced by it moves in the opposite direction, making the air migration asymmetric.

3. Results and Discussion

3.1 Smoke Visualisations

Figures 2 – 7 show the side- and top-view smoke visualizations for the single hinged and single sliding doors. Each figure shows a series of still images (A - D) obtained from the recorded videos. Subfigure A depicts the quiescent situation before the door was opened, B the airflow through the doorway after the door has opened completely, C the combined effect of the door and manikin (in motion) and (D) the situation after the manikin has stopped and the door closed behind it.

Figure 2 (hinged door anteroom side-view) shows that the hinged door creates a pronounced flow through the doorway and that the smoke spreads far inside the room. The effect of the manikin passage is difficult to determine because the drastic influence of the door itself overshadows the impact of the passage. However, after the manikin has stopped, the air dragged in the wake spreads around the room indicating that a significant amount of air was carried by the manikin from the isolation room. After the motion (of the door and manikin) has stopped, the air movement slowly settles down and static conditions take over again.

Figure 3 depicts the hinged door operation seen from top to bottom (in anteroom). The smoke can be seen to spread effectively also horizontally throughout the room. Otherwise the airflow patterns are similar to the side-view situation (pronounced flow merely by the door, combined effect of the door and manikin difficult to distinguish and smoke is convected towards the end of the room).

Figure 4 shows the airflow patterns on the isolation room side (side-view) of the single hinged door. The door creates a door vortex in the doorway (as seen by

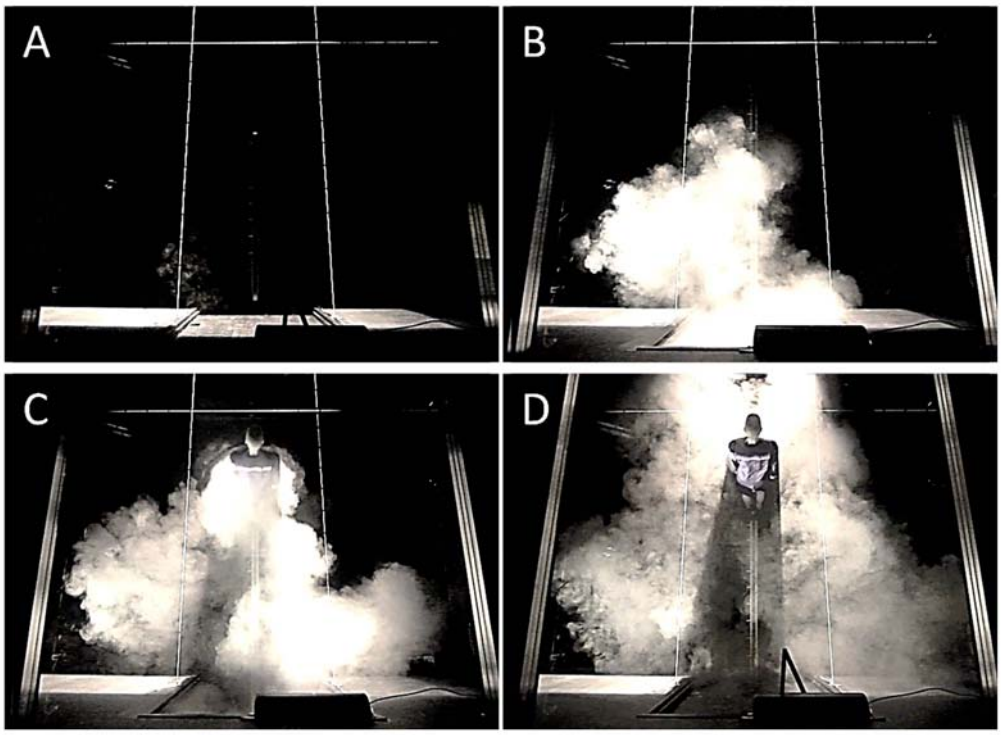

Figure 3. Smoke visualization (anteroom top-view) of the airflow patterns across the doorway generated by the single hinged door and the manikin passage.

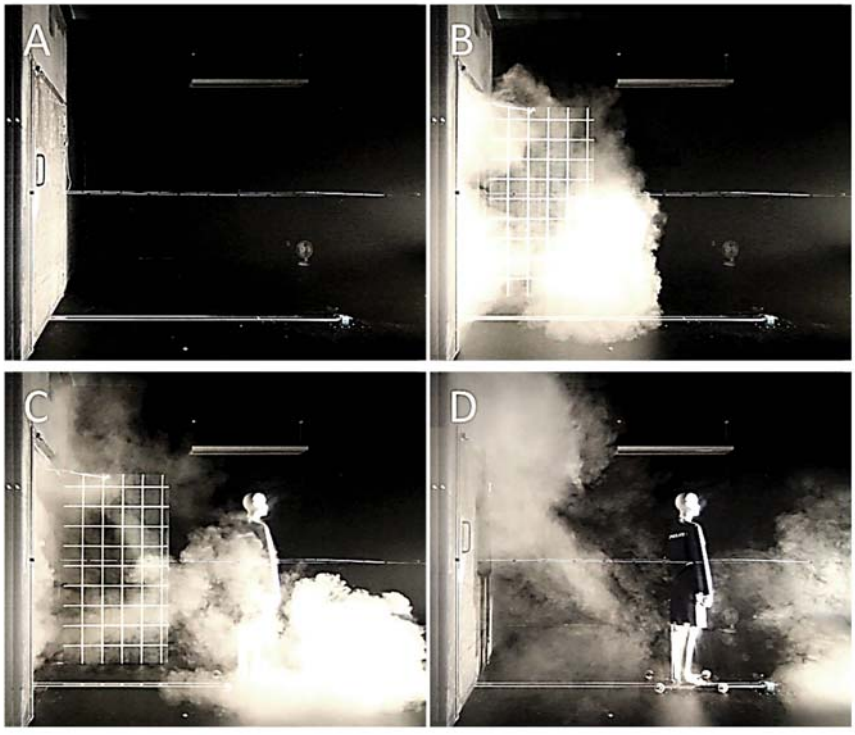

Figure 4. Smoke visualization (isolation room side-view) of the airflow patterns across the doorway generated by the single hinged door and the manikin passage.

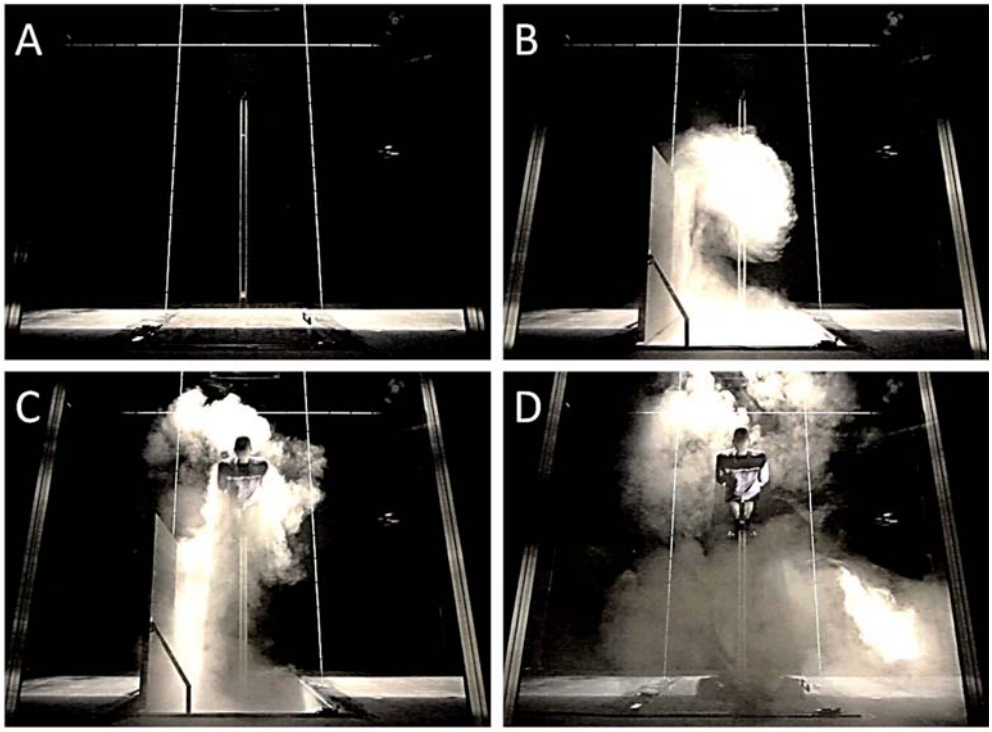

Figure 5. Smoke visualization (isolation room top-view) of the airflow patterns across the doorway generated by the single hinged door and the manikin passage.

the smoke next to the door). The vortex disengages from the door and continues to move across the room. The effect of the manikin (in motion) and the wake are again difficult to distinguish (covered by the effect of the door). The door vortex can be seen moving in front of the manikin (flattened on its way). The closing door pushes the smoke from the doorway towards the viewer. The closing door also creates another door vortex behind it, the remnants of which can be seen behind the manikin.

Figure 5 illustrates the situation seen from top to bottom on the isolation room side of the doorway. Now the door vortex generated by the opening door can be seen more clearly next to the door. In the next image it can be seen moving in front of the manikin. Again, the effect of the moving manikin is difficult to distinguish (masked by the effect of the door). Now the flow caused by the closing door can be seen on the right side of the door.

Anteroom side-view of the smoke visualizations for the single sliding door is presented in Figure 6. The sliding door causes merely a modest flow through the doorway and the smoke is spread only in close proximity to the doorway. The wake behind the manikin can easily be detected. The smoke in the wake continues moving towards the end of the room after the manikin has stopped.

Figure 7 shows the smoke visualization for the sliding door seen from top to bottom in the anteroom. Only modest horizontal dispersion can be seen. The wake is clearly detectable. The wake spreads over a wide horizontal area after the manikin has stopped. Visualizations for the sliding door are shown only from one side of the doorway because the geometry and the flow patterns were essentially similar on both sides.

There are no published experimental visualizations made in full-scale to compare the results against. However, there are some made with small-scale models and using CFD simulation methods. The small-scale water model visualizations by Tang et al (2013) were made using an identical 1:10 scale model as used in this study. Their visualizations show that sliding doors produce far less disturbance and air exchange across the doorway than hinged doors. This can be seen in this study as well, for

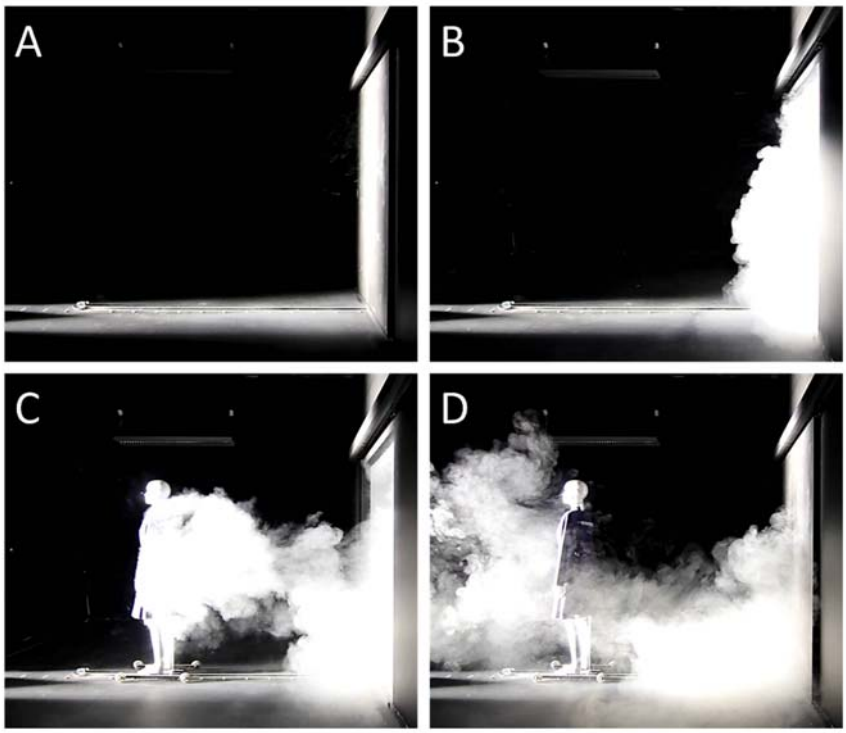

Figure 6. Smoke visualization (anteroom side-view) of the airflow patterns across the doorway generated by the sliding door and the manikin passage.

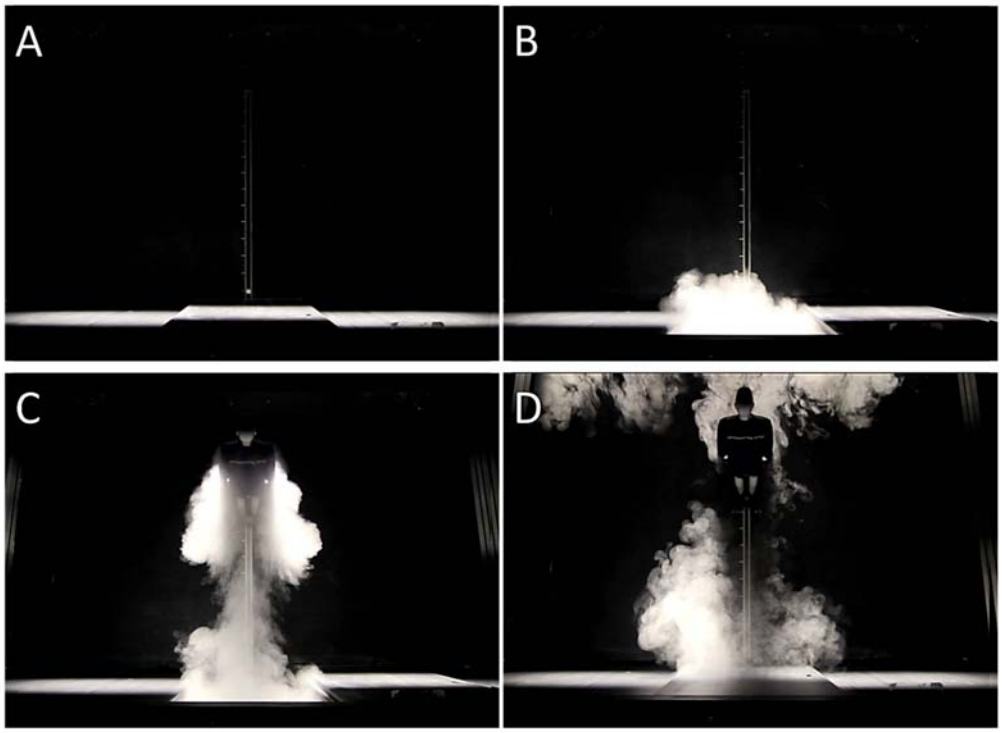

Figure 7. Smoke visualization (anteroom top-view) of the airflow patterns across the doorway generated by the sliding door and the manikin passage.

Table 1. Tracer gas measurement results (averages and standard deviations).

Door type	Opening time	Hold open time	Closing time	Total cycle time	Passage	Avg. temp. diff.	Avg. airflow (m^3) 1->2	Standard deviation 1->2	Avg. airflow (m^3) 2->1	Standard deviation 2->1
The door type:										
Hinged*	3	8	5.4	16.4	-	-	**1.30**	0.16	**1.39**	0.12
Sliding*	3	8	5.4	16.4	-	-	**0.54**	0.04	**0.56**	0.07
With different opening sizes:										
Hinged**	2.8	8	4.9	15.7	-	-	-	-	**1.16**	0.15
Sliding**	1.8	8	3.3	13.1	-	-	-	-	**0.34**	0.04
With different opening times:										
Hinged*	3	2.1	5.4	10.5	-	-	-	-	**1.37**	0.09
Sliding*	3	2.1	5.4	10.5	-	-	-	-	**0.29**	0.06
Hinged*	8	2.1	14.5	24.6	-	-	-	-	**1.63**	0.10
Sliding*	8	2.1	14.5	24.6	-	-	-	-	**0.75**	0.06
Hinged*	4.8	8	8.7	21.5	-	-	-	-	**1.77**	0.17
Sliding*	4.8	8	8.7	21.5	-	-	-	-	**0.67**	0.09
Hinged*	8	8	14.5	30.5	-	-	-	-	**1.81**	0.16
Sliding*	8	8	14.5	30.5	-	-	-	-	**0.93**	0.04
With different hold-open times:										
Hinged*	3	13.5	5.4	21.9	-	-	-	-	**1.75**	0.12
Sliding*	3	13.5	5.4	21.9	-	-	-	-	-	-
Hinged*	3	19	5.4	27.4	-	-	-	-	**1.61**	0.14
Sliding*	3	19	5.4	27.4	-	-	-	-	**0.91**	0.10
Hinged*	3	24.8	5.4	33.2	-	-	-	-	**2.42**	0.24
Sliding*	3	23.8	5.4	32.2	-	-	-	-	**1.13**	0.07
With 2°C temperature difference:										
Hinged*	3	8	5.4	16.4	-	2.02	-	-	**1.96**	0.13
Sliding*	3	8	5.4	16.4	-	2.22	-	-	**2.26**	0.10
With passage:										
Hinged*	3	8	5.4	16.4	Both dir.	-	-	-	**1.65**	0.31
Sliding*	3	8	5.4	16.4	Both dir.	-	-	-	**0.92**	0.08
Hinged*	3	8	5.4	16.4	2->1	-	-	-	**1.93**	0.09
Sliding*	3	8	5.4	16.4	2->1	-	-	-	**0.98**	0.06
Hinged*	3	8	5.4	16.4	1->2	-	-	-	**1.37**	0.11
Sliding*	3	8	5.4	16.4	1->2	-	-	-	**0.87**	0.05

* Gap size 90 degrees with hinged door and 1.10 m with sliding door

** Gap size 45 degrees with hinged door and 0.55 m with sliding door

instance comparing Figures 2B and 6B. Tang et al (2013) noticed also that the relative effect of the passage was clearer with sliding doors than with hinged ones. This phenomenon is present also in this study (compare Figures 3C and 7C for example). These findings support our results and also justify the scaling methods and application of the small-scale water model.

Choi and Edwards (2008) used time-accurate CFD simulation methods to model (in full-scale) a manikin walking through an open doorway (in the absence of door and ventilation). Their two-room model was similar to our isolation room model. Their visualization of room to room contaminant transport produced very similar effects as noticed in the visualizations shown here.

In a follow up study, Choi and Edwards (2012) utilized a more complex geometry and simulated a manikin walking from dirty area to clean area through a small chamber fitted with two hinged or two sliding doors. Although the effects of human thermal plume and ventilation were included, the visualizations looked very realistic and similar to the ones presented here, despite the differences in the geometry.

3.2 Tracer Gas Measurements

Tracer gas measurements were made in order to quantify the air exchange volume through the doorway. The results (averages and standard deviations) for both door types are shown in Table 1. The effects of different factors are discussed below in several subsections.

3.2.1 Door Type

The first subsection of Table 1 shows the air exchange volume induced by the two door types without passage. The sliding door generated significantly less air exchange through the doorway than the single hinged door. The results are visualized in the left side of Figure 8. The distinct difference between the two different door types is not surprising as the smoke visualizations shown in Figures 2 - 7 already suggest it. In addition, Hayden et al (1998) have reported similar findings earlier (although utilizing ventilation and pressure difference).

A comparison was made between the two flow directions to test the measurement system and to see whether equal air volumes were transferred to both directions through the doorway (as assumed based on the closed system hypothesis). As can be seen from the left side of Figure 8, the averages are close to the dashed line which reflects equal air exchange in both directions across the doorway. This justifies the assumption of a closed system and hence from now on only the results for air escaping the isolation room will be shown and discussed.

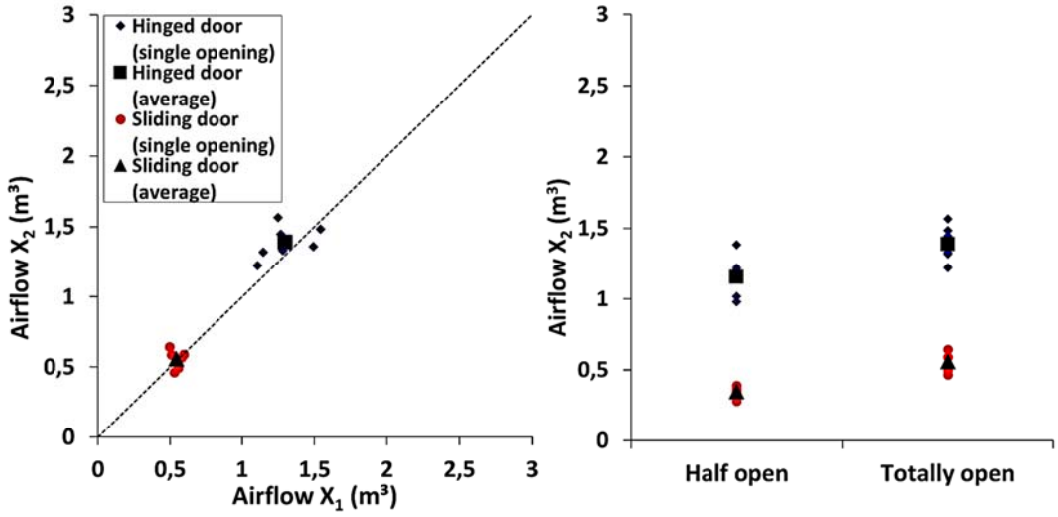

Figure 8. Tracer gas measurement results. The amounts of airflow to opposite directions (on the left) and the effect of door opening gap (on the right) for both door types without passage. X2 denotes the air volume migrating from the isolation room to the anteroom.

3.2.2 Reduced Opening Size

The second subsection of Table 1 (from above) shows the tracer gas results for a half way opened doorway. The results are visualized and compared to a fully opened doorway in the right side of Figure 8. The reduction of the opening gap to half cuts the flow across the doorway by 17% and 39% for hinged and sliding doors respectively. However, due to limitations of the hinged door operator, the opening time was slightly longer than for the sliding door which may affect the hinged door results.

There is no clear consensus what factors govern the air exchange through the doorway although one seems to be the swept volume of the door. Based on the small-scale water model studies by Eames et al (2009) and Fontana and Quintino (2014) the exchanged air volume is comparable to the swept volume of the door. On the other hand, Kiel and Wilson (1989) found (by using a small-scale water model without ventilation) the typical exchange volume to be only 50% of the swept volume of the door.

In our case the measured air volume exchange was about 70% of the swept volume of the fully opened single hinged door. For half opened single hinged door the measured volume exchange was about 118% of the swept volume. Thus the dependency of the air volume exchange on the swept volume of the door is not clear. Indeed, further investigation is needed to cover the effect thoroughly.

3.2.3 Door Opening Times

The tracer gas measurement results for different door opening times are shown in the third subsection of Table 1. All the different opening time results are visualized in the top left corner of Figure 9. It seems that the longer the opening time the greater the air exchange through the doorway for both door types. This can be seen for both door hold open times (i.e. 2 s and 8 s). The increase for the sliding door seems to be almost linear.

The result is slightly surprising as other studies have reported different, even opposite findings. For instance, Hayden et al (1998) concluded in their study that increasing the hinged door opening time from 5 s to 8 s (and closing time from 8 s to 12 s correspondingly) the air volume migration through the doorway (hold-open time constant 2 s) showed no significant effect. However, they carried out their investigation under the influence of ventilation and pressure difference between the rooms and it might well be that when applying high ventilation rates the room flow patterns mask the actual effect of the door speed and no significant effect can be observed.

On the other hand, Kiel and Wilson (1989) found out that the speed of the hinged door increases the volume exchange across the doorway. However, they carried out the experiments through the outer door of a test house in a small-scale water model. Additionally the hold-open time in their experiments was apparently only 1.0 s, hence caution should be used while comparing their results with those presented here.

3.2.4 Door Hold-Open Times

Results for tracer gas measurements with different door hold-open times are shown in the fourth subsection of Table 1. The results are illustrated in the top right corner of Figure 9. The exchange volume through the doorway increases with the hold-open time. This is clearer with the sliding door, which indicates a linear trend with hold-open time. Similar findings were reported by Hathway et al (2014) for a hinged door by using a small-scale water model without ventilation.

The effect of door hold-open time is rather natural, as the door (the only driving force in our isothermal case) sets the air in motion and as long as there is momentum on the doorway the air exchange through the doorway continues. Eventually the momentum will die out and then the total volume passing through the doorway no longer increases. However, this saturation was not detected with the hold-open times used in this study. Also, very long hold-open times are unrealistic considering typical door openings in hospital isolation rooms and thus are not covered in this study.

3.2.4 Door Total Cycle Times

The impact of the door total cycle time is presented in the bottom left corner of Figure 9. This includes all the previously presented measurements for totally opened doorways. Hence it includes combinations of different opening and hold open times. Nevertheless, the trend is clear, the longer the total cycle time the greater the air exchange through the doorway for both door types.

This can now explain the increasing air exchange across the doorway with opening time. The slower

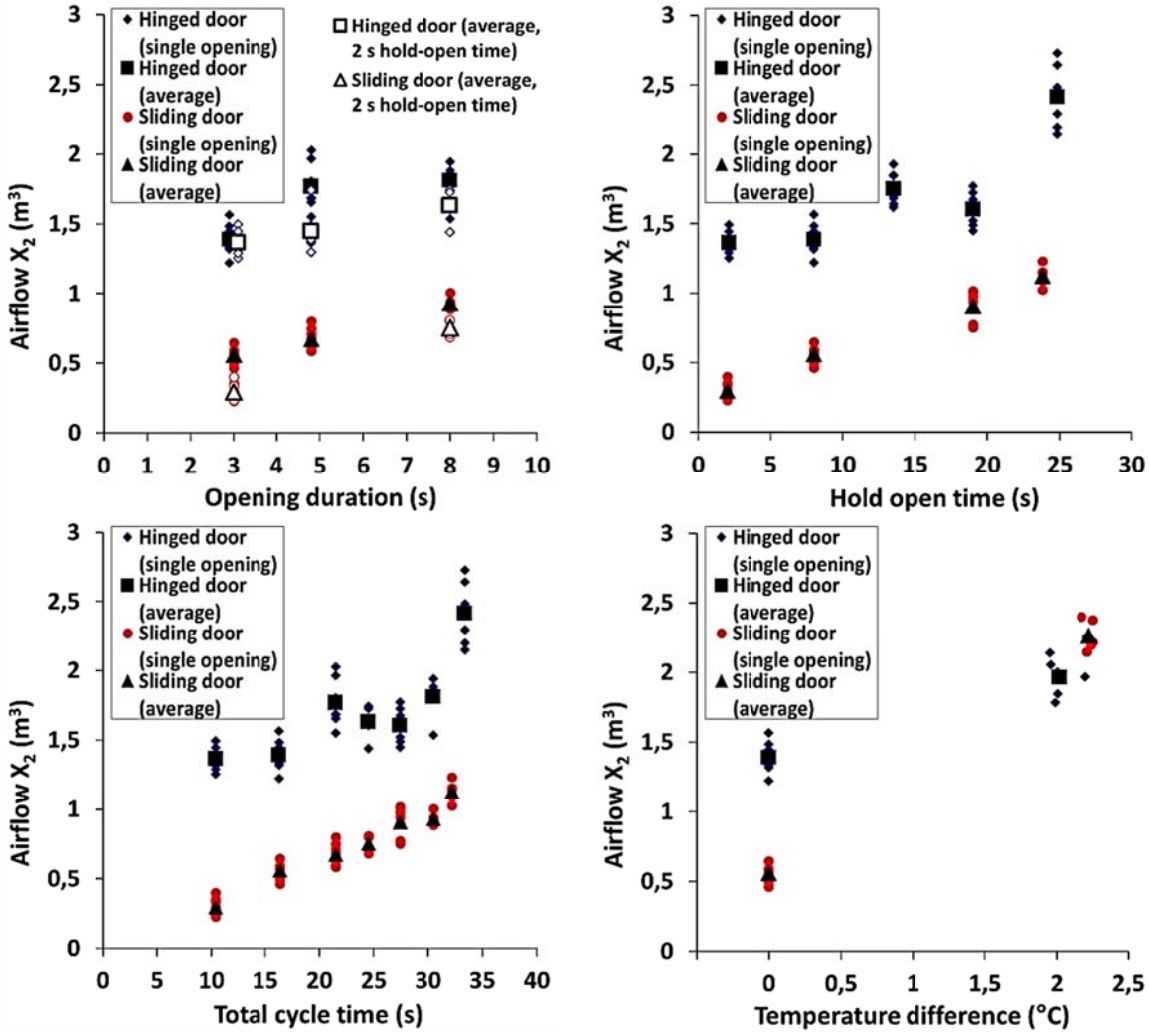

Figure 9. Tracer gas measurements results. The effect of opening time (top left corner), hold-open time (top right corner), total cycle time (bottom left corner) and 2 °C temperature difference on the airflow through the doorway (for both door types without passage) (bottom right corner). X_2 denotes the air volume migrating from the isolation room to the anteroom.

the door opening time, the longer the total cycle time and thus the greater the airflow through the doorway. Yet, this was not seen in the studies by Kiel and Wilson (1989) and Hayden et al (1998) when they varied opening times and kept the hold-open time constant. Additional experiments when varying the door opening times while keeping the total cycle time constant are needed to confirm this hypothesis.

3.2.5 Temperature Difference

The results of the tracer gas measurements for 2 °C temperature difference for both door types are shown in the fifth subsection of Table 1. The results are visualized in Figure 9 bottom right corner. As can be seen from the table and from the figure the volume migration through the doorway increases significantly even with this rather small temperature difference. The increase is far more drastic for the sliding door (303%) than for the hinged door (41%). The strong flow induced by the opening action of the hinged door can reduce the effect of the temperature driven airflows across the doorway at the beginning of the door operation. After the initial effect of the hinged door declines, the temperature difference starts to impact the air exchange between the rooms. This cannot be observed with the sliding

door as the door induced flows are significantly weaker and the temperature difference driven flow starts to dominate early on. However, as the total air exchange with both door types are similar (for $\Delta T = 2$ °C), the acceleration time of temperature difference driven flow for hinged door is compensated by the pumping action. Similar findings were reported by Kiel and Wilson (1989) using a full size test house and a small-scale water model.

3.2.6 Passage and Its Direction

The tracer gas measurement results with the manikin passage for both door types are shown in the last subsection of Table 1. The results are illustrated in Figure 10. The effect of the passage is significant and clear for both door types although more distinct for the sliding door. The data dispersion, especially for the passage through the single hinged door, is notable. Based on the sliding door measurements (less disturbance caused by the door itself), the additional average air exchange generated by passage (to both directions) is 0.36 m^3. According to smoke visualizations (Figures 2 – 7), the air is dragged through the doorway in the wake of the manikin. Tang et al (2006) has estimated the wake flow rate to be around 0.08 – 0.23 m^3/s. Eames et al (2009) refined this estimate to be 0.4 m^3/s. The door hold open time used in this study (in connection with passage) would then lead to a total volume transfer produced by the passage alone to be 3.2 m^3. Even without considering the effect of the door one can notice that these wake flow rate assessments are overestimates and do not correspond well with the measurements shown here. There are several reasons for this: the estimated drag coefficient of the human body (~1) might be different or the flow rate might die out faster than expected. Further analysis is needed to match the theoretical values with the measurement. However, this was beyond the scope of the current study.

Hayden et al (1998) concluded that passage considerably increased the air volume migration through the doorway (and was a dominant factor with sliding door), but there was no significant difference in the migrating air volumes between the hinged and sliding doors when passage was involved. However, this study found a significant difference between hinged and sliding doors even when passage was involved. The results are not directly comparable because Hayden et al (1998) carried out the experiments with ventilation and pressure difference. Especially the ventilation might induce flow patterns which drastically modify the situation and hence the air exchange between the rooms.

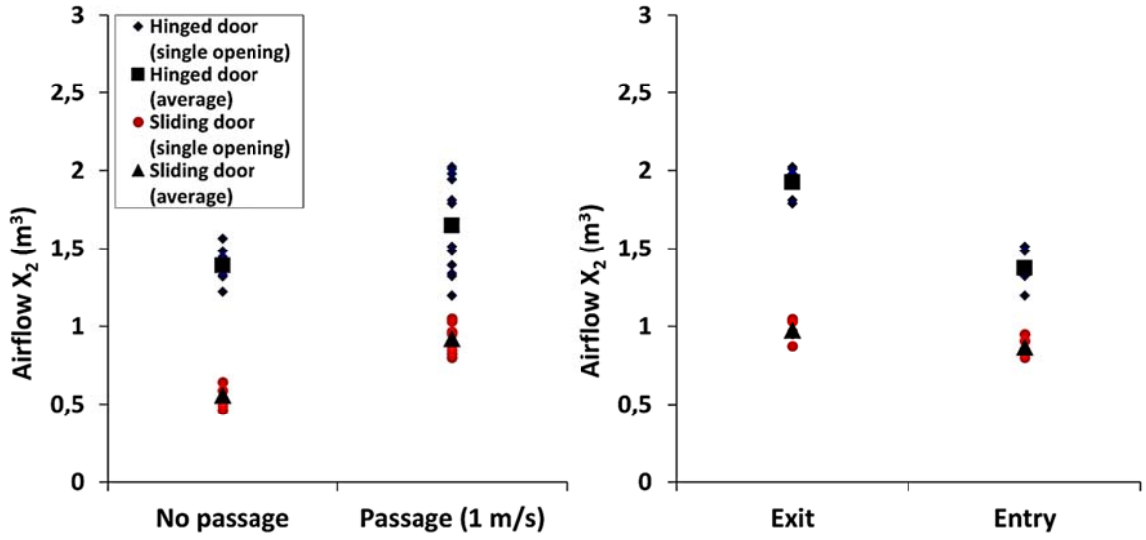

Figure 10. Tracer gas measurement results. The effect of passage (on the left) and passage direction (on the right) on the airflow through the doorway (for both door types). X_2 denotes the air volume migrating from the isolation room to the anteroom.

Studies carried out in real hospital environments have also reported elevated concentrations of tracer gas, particles etc. in the anteroom/corridor after a health care provider exits from the isolation room (Rydock and Eian 2004; Adams et al 2011). However, they were mostly carried out with hinged doors which indicates that they are currently the most utilized door solutions for isolation rooms. The results shown here together with visualizations carried out by Tang et al (2013) address the need for at least considering utilizing sliding doors to reduce air escaping the isolation room during door operation. However it is recognized that transition to sliding doors might be challenging due to strict space demands (especially in small anterooms). Also additional maintenance costs to avoid breakdown could be needed since sliding doors are typically automatic. However, sliding doors should be at least considered when constructing new hospitals or renovating old ones.

On the right side of Figure 10, the effect of passage is broken down to two categories by passage direction (i.e. exit and entry). Passage (exit) against the single hinged door opening direction amplifies the volume exchange across the doorway by 40% compared to passage (entry) parallel to the door opening direction. No substantial difference was found for the sliding door set-up.

By contrast, in studies carried out in a non-quiescent environment, no notable effects of passage direction have been reported. Kokkonen et al (2014) stated that the movement direction of a health care worker did not cause any clear effect on tracer transfer through hinged doors. Hayden et al (1998) similarly concluded that the entry or exit (i.e. passage direction) showed no substantial effect on air volume migration across the doorway. Hence it seems that high ventilation rates affect the passage induced flows cancelling the consequences of passage direction. In order to verify this it is necessary to carry out experiments with realistic ventilation rates and pressure differences.

The manikin used in this study was not a thermal manikin as its surface was not heated. The practical impacts of the thermal plume are considered to be limited as indicated in a study by Wu and Gao (2014), in which they studied the effect of body motion induced wake flow on contaminant dispersion with and without a thermal plume. They pointed out (by using CFD models) that the effect of the thermal plume on wake flow is dependent on moving speed. For a manikin moving velocity around 0.2 m/s the thermal plume near the manikin body was comparable to the wake flow. For manikin moving velocities over 0.4 m/s the wake flow dominates over the thermal flows induced by the body heat and thus the influence of the thermal plume can be neglected. Additionally the results by Licina et al (2015) support the findings of Wu and Gao (2014). Licina et al (2015) studied the effect of room ventilation flows on the human convective boundary layer. They concluded that horizontal flow of 0.425 m/s towards the manikin completely replaced the upward convective boundary layer flow with air flows parallel to horizontal flow. Hence it seems that in our case, as the manikin was moving 1 m/s, the convective boundary layer does not affect the results significantly.

However, the thermal manikin can heat up the room slightly (compared to the other room) and the resulting temperature difference might increase the air exchange between the rooms during the door operation. Nevertheless, the temperature difference induced air exchange between the rooms is covered by our study and can be estimated from Figure 9 (bottom right corner) and Table 1.

Although the focus of this study was on airflows between the isolation and anteroom it should be noted that in real-life situations airborne contaminants transferred to the anteroom (during entry and subsequent exit from the isolation room) will be dispersed to the corridor when leaving the anteroom. Although this propagation to the wider corridor area was not measured in this study it has been estimated by Kokkonen et al (2014) to be around 0.05 – 0.20 m^3 and hence significant.

In practice the anteroom size is smaller than the isolation room. However, in our model the rooms were made symmetrical in order to study the airflow patterns generated by the manikin exiting the door in either direction. According to Hayden et al (1998) the anteroom size affects the amount of tracer gas migrating from the isolation room to the corridor, smaller reducing and larger increasing the migration. On the other hand, Kiel and Wilson (1989) found out that air exchange through the outer door (single hinged door without passage) of a small house (with different indoor-outdoor temperature differences) was not significantly affected by the room size or layout. Hence it seems that the effect of the room size on the air exchange between spaces is not well established and needs detailed study in the future.

Clearly there is a need to repeat our measurements for realistic isolation room conditions (i.e. with realistic ventilation rates and pressure differences) to see whether the findings reported without ventilation would still be valid. However, the purpose of this baseline study was to examine the door and passage produced effects without the severely masking influence of high ventilation rates which would have made it impossible to explore the distinct results of different factors.

4. Conclusions

In this study hinged and sliding door induced flows and air exchange between an isolation room and an anteroom were examined in still air (i.e. without ventilation) for different door operation parameters, including passage.

Based on smoke visualizations both door types were found to produce a detectable airflow through the doorway and hence to be able to transfer possibly pathogen laden air from the isolation room into the anteroom and possibly to the corridor. However, the sliding door was found to generate notably smaller and tardy flow compared to the hinged door. The passage of a person through the door induced flows were notable for both door types but easier to distinguish and relatively more significant for the sliding door.

Based on the tracer gas measurements the exchange volume was found to range between 0.3 m^3 – 2.3 m^3 for a sliding door and between 1.2 m^3 – 2.4 m^3 with a hinged door (depending on the experimental parameters). In each studied case (temperature difference measurements aside) the exchange volume was found to be significantly lower for the sliding door than for the hinged door. The air exchange between the isolation room and the anteroom was found to increase notably while increasing the hold-open, total cycle and opening times with both door types. Also, the 2 °C temperature difference between the rooms was found to increase the air exchange substantially. This was relatively more significant for the sliding door.

Passage was found to notably increase the air volume transfer through the doorway for both door types. Based on the sliding door measurements, the exchange volume induced by the passage was found to be about 0.4 m^3. The passage direction was found to significantly influence the exchange volume with the hinged door (greater exchange when moving against the opening direction). When exiting (entering) the isolation room the total air volume transfer induced by the combined effect of door and passage was found to be 1.9 m^3 (1.4 m^3) with the hinged door and 1.0 m^3 (0.9 m^3) with the sliding door. Hence sliding door operation induces substantially smaller volume exchange through the doorway compared to the hinged door.

In the future, the performance of the hinged and sliding doors will be compared under the influence of realistic ventilation rates and pressure differences in combination with passage.

Acknowledgement

Funding for this study was provided by the Finnish Funding Agency for Technology and Innovation (TEKES). It was part of a project co-funded by TEKES and A*STAR (Agency for Science, Technology and Research). Additionally the authors would like to thank Jarkko Hakala and David Oliva for their efforts and help when constructing the full-scale isolation room model.

References

Adams NJ, Johnson D and Lynch R: (2011) “The effect of pressure differential and care provider movement on airborne infectious isolation room containment effectiveness”, *Am. J. Infect. Control*, **39**, pp91-97.

Choi JI and Edwards JR: (2008) “Large eddy simulation and zonal modeling of human-induced contaminant transport”, *Indoor Air*, **18**, pp233-249.

Choi JI and Edwards JR: (2012) “Large-eddy simulation of human-induced contaminant transport in room compartments”, *Indoor Air*, **22**, pp77-87.

Eames I, Shoaib D, Klettner CA and Taban V: (2009) “Movement of airborne contaminants in a hospital isolation room”, *J. R. Soc. Interface*, 6 (Suppl 6), pp757-766.

Fontana L and Quintino A: (2014) “Experimental analysis of the transport of airborne contaminants between adjacent rooms at different pressure due to the door opening”, *Building and Environment*, **81**, pp81-91.

Fraser VJ, Johnson K, Primack J, Jones M, Medoff G and Dunagan WC: (1993) "Evaluation of rooms with negative pressure ventilation used for respiratory isolation in seven Midwestern hospitals", *Infect. Control Hosp. Epidemiol*., **14**, pp623-627.

Hathway A, Papakonstantis I, Konuah AB and Brevis W: (2014) "Towards understanding the role of human activity on indoor air flows: A case study of door motion based on both field and experimental activities", In: *Proceedings of Indoor Air 2014, 13th International Conference on Indoor Air Quality and Climate*, 7 – 12 July, Hong Kong, China.

Hayden CS II, Johnston O, Hughes R and Jensen PA: (1998) "Air volume migration from negative pressure isolation rooms during entry/exit", *Appl. Occup. Environ. Hygiene*, **13**, (7), pp518-527.

Hyttinen M, Rautio A, Pasanen P, Reponen T, Earnest SG, Streifel A and Kalliokoski P: (2011) "Airborne infection isolation rooms – A review of experimental studies", *Indoor and Built Environment*, 20, (6), pp584-594.

Kiel DE and Wilson DL: (1989) "Combining door swing pumping with density driven flow", *ASHRAE Trans*, **95**, pp590-599.

Kokkonen A, Hyttinen M, Holopainen R, Salmi K and Pasanen P: (2014) "Performance testing of engineering controls of airborne infection isolation rooms by tracer gas techniques", *Indoor and Built Environment*, **23**, (7), pp994-1001.

Licina D, Melikov A, Sekhar C and Tham KW: (2015). "Human convective boundary layer and its interaction with room ventilation flow", *Indoor Air,* doi:10.1111/ina.12120. **25**, (1), pp21-35.

Martin, "Particle size, fluid density and refractive index values", revision A, http://www.martinpro.com/service/showpage.asp?id=8074&tit=Pro+Smoke+Super+%28ZR+mix%29&thisprod=prosmokesuperzrmix, accessed 9.1.2014.

Rice N, Streifel A and Vesley D: (2001) "An evaluation of hospital special-ventilation-room pressures", *Infect. Control Hosp. Epidemiol*., **22**, (1), pp19-23.

Rydock JP and Eian PK: (2004) "Containment testing of isolation rooms", *Journal of Hospital Infection*, **57**, pp228-232.

Saravia SA, Raynor PC nd Streifel AJ: (2007) "A performance assessment of airborne infection isolation rooms", *Am. J. Infect. Control*, **35**, pp324-331.

Tang JW, Li Y, Eames I, Chan PKS and Ridgway GL: (2006) "Factors involved in the aerosol transmission of infection and control of ventilation in healthcare premises". *Journal of Hospital Infection*, **64**, pp100-114.

Tang JW, Eames I, Li Y, Taha YA, Wilson P, Bellingan G, Ward KN and Breuer J: (2005) "Door-opening motion can potentially lead to a transient breakdown in negative-pressure isolation conditions: the importance of vorticity and buoyancy airflows". *Journal of Hospital Infection*, **61**, pp283-286.

Tang JW, Nicolle A, Pantelic J, Klettner C, Su R, Kalliomäki P, Saarinen P, Koskela H, Reijula K, Mustakallio P, Cheong DKW, Sekhar C and Tham KW: (2013) "Different types of door-opening motions as contributing factors to containment failures in hospital isolation rooms". *PLoS One,* **8**, (6), e66663. doi:10.1371/journal.pone.0066663.

Wu Y and Gao N: (2014) "The dynamics of the body motion induced wake flow and its effects on the contaminant dispersion", *Building and Environment*, **82**, pp63-74.